

Quasiparticle coherence and the nature of the metal-insulator phase transition in Na_xCoO_2

D. Qian,¹ L. Wray,¹ D. Hsieh,¹ D. Wu,² J.L. Luo,² N.L. Wang,²
A. Fedorov,³ A. Kuprin,³ R.J. Cava,⁴ L. Viciu,⁴ and M.Z. Hasan^{1,5}

¹*Department of Physics, Joseph Henry Laboratories of Physics, Princeton University, Princeton, NJ 08544*

²*Institute of Physics, Chinese Academy of Sciences, Beijing 100080, China*

³*Advanced Light Source, Lawrence Berkeley Laboratory, Berkeley, Ca 94305*

⁴*Department of Chemistry, Princeton University, Princeton, NJ 08544*

⁵*Princeton Center for Complex Materials, Princeton University, Princeton, NJ 08544*

(Dated: August 12, 2021)

Layered cobaltates embody novel realizations of correlated quantum matter on a spin-1/2 triangular lattice. We report a high-resolution systematic photoemission study of the insulating cobaltates ($\text{Na}_{1/2}\text{CoO}_2$ and $\text{K}_{1/2}\text{CoO}_2$). Observation of single-particle gap opening and band-folding provides direct evidence of anisotropic particle-hole instability on the Fermi surface due to its unique topology. Kinematic overlap of the measured Fermi surface is observed with the $\sqrt{3}\times\sqrt{3}$ cobalt charge-order Brillouin zone near $x=1/3$ but not at $x=1/2$ where insulating transition is actually observed. Unlike conventional density-waves, charge-stripes or band insulators, the on-set of the gap depends on the quasiparticle's quantum coherence which is found to occur well below the disorder-order symmetry breaking temperature of the crystal (the first known example of its kind).

PACS numbers: 71.27.+a, 71.20.Be, 71.30.+h, 73.20.At, 74.70.b

Strong electron-electron interaction (Mott physics) is known to be the origin of metal to insulator transitions as a function of doping and temperature in many oxides[1]. Such systems exhibit strong quantum effects if electron transport occurs in lower dimensions and the underlying band is half-filled (spin-1/2). Recently discovered Na_xCoO_2 is the first realization of a spin-1/2 doped Mott insulator on a triangular lattice [2, 3, 4]. This system exhibits not only superconductivity [5] and spin-dependent thermopower [6] but also antiferromagnetism and spin-density-wave phases[2] as well as an unusual metal-insulator transition [2, 3, 4, 7, 8]. Most Mott systems exhibit insulating phases while doped near the natural commensurate values of the underlying lattice [1]. Surprisingly, the insulating state in cobaltates is observed near the $x=1/2$ doping which is not a natural commensurate value ($x = 1/3$ or $2/3$) of the triangular lattice. This remains an unsolved issue to this date. In this Letter, we report the microscopic electron dynamics in the vicinity of the metal-insulator phase transition in Na_xCoO_2 which reveals that the insulating state in cobaltates is due to an anisotropic particle-hole instability on the Fermi surface resulting from its unique momentum-space topology with respect to the Na^+ charge-order. However, unlike the conventional charge-density-waves, the on-set of the insulating gap (order parameter) is related to the energy-scale of the emergence of quasiparticle coherence instead of the disorder to order symmetry breaking temperature which is the first known example of its kind.

Electron[2, 3], neutron [4], infrared (IR)[7], Shubnikov-de Haas (SdH) [9] and NMR measurements[10] have been used to study the insulating state. However, ARPES studies have so far only been carried out on the metallic

cobaltates[11]. In this Letter, we report a single-particle study of the cobaltate insulator for the first time. High

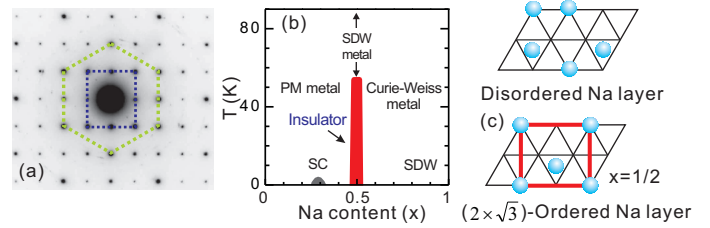


FIG. 1: **Phase transitions in Na_xCoO_2** : (a) Electron diffraction image along the [001] symmetry axis. The rectangular supercell is observed due to the Na^+ charge ordering (Wigner crystallization). (b) Phase diagram of Na_xCoO_2 [2]. Metal-insulator phase transitions are observed in doping near $x=1/2$ where (c) Na layer undergoes a disorder to order transition well above the room temperature[2, 3, 4].

quality single crystals of $\text{Na}_{1/2}\text{CoO}_2$ and $\text{K}_{1/2}\text{CoO}_2$ and nearby dopings were grown by the floating zone and flux methods respectively. Na concentration near 0.5 (0.49 to 0.51) was achieved by post-growth deintercalation whereas K samples could be naturally grown with $x=0.5$ (0.47 to 0.53) doping. Insulating states with two characteristic resistivity upturns around 50K and 25K in Na-samples and 60K and 20K in K-samples (Fig.5(a)) were observed. K-based materials were used for better surface retention of doping. No surface state was observed. High quality of both Na and K samples allowed us to observe clear band-folding and gap. Spectroscopic measurements were performed at the Adv. Light Source. The data were collected with He I (21.2eV), 30 eV or 60 eV photons with better than 8, 12 or 10 meV energy resolution and an an-

gular resolution better than 2% of the Brillouin zone at Beamlines 12.0.1 and 10.0.1 using Scienta analyzers with chamber pressures better than 4×10^{-11} torr.

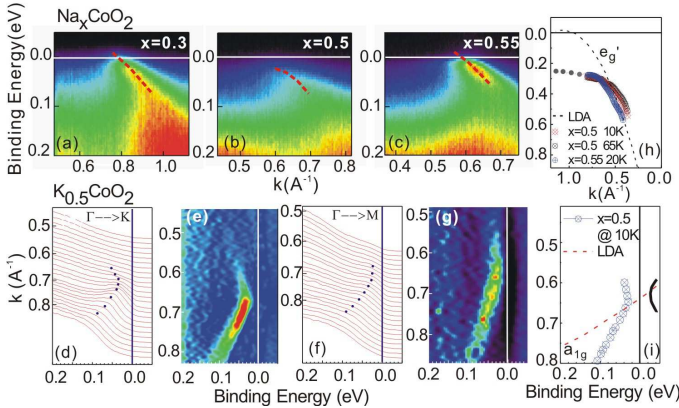


FIG. 2: **Quasiparticle Dynamics:** Single-particle removal spectra of samples with doping (a) $x=0.3$, (b) $x=0.5$ and (c) $x=0.55$. (d) and (e) show spectra and color images (SDI) along $\Gamma \rightarrow K$ while (f) and (g) are spectra measured along $\Gamma \rightarrow M$. (h) Doping and temperature dependence of e_g' band dispersions in the vicinity of $x=0.5$ which show no changes. (i) Experimental band dispersion is compared with LDA theory (dotted line)[12]. The measured band is less dispersive. It exhibits folding and a gap opens at the Fermi level.

No measurable sign of sample charging was observed down to 10K. No appreciable loss of Na-2p (or K-3p) peak intensity was observed within the probe-depth of ARPES and within a few hours of cleaving in UHV. Such care has been quite crucial in observing the energy gap since a change of doping ($>3\%$) or aging turns the sample into a metal with a large Fermi surface (FS). Measured FS area further provided an internal check for changes in effective doping on the surface. Rotating analyzers allowed us to polarization select the a_{1g} -band states (under P-geometry) and e_g' -band states (S-geometry) distinctively.

Fig.-2(a-c) shows the quasiparticle dispersion as the system approaches the insulating phase from either side of the doping phase diagram (namely $x=0.3$, $x=0.5$ and $x=0.55$) within 200meV of the electron binding energies at 20K. Only in $x=0.5$ samples is spectral weight suppression observed at low temperature. The gap behavior is seen in the energy distribution curves in Fig-2(d-g). The $x=0.5$ samples show a clear pull-back of the quasiparticle along the high symmetry cut $\Gamma \rightarrow K$. A spectral gap is also observed along $\Gamma \rightarrow M$ but the folding behavior is less prominent. These quasiparticles emerge from the a_{1g} -like states. We have carefully monitored changes at the e_g' bands under S-geometry as they are predicted to be involved in the ordering transition[13, 14]. The e_g' band is found to be fully gapped and hardly showed any temperature or doping dependence (Fig.-2(h)). Therefore we conclude that the insulating gap opens by the

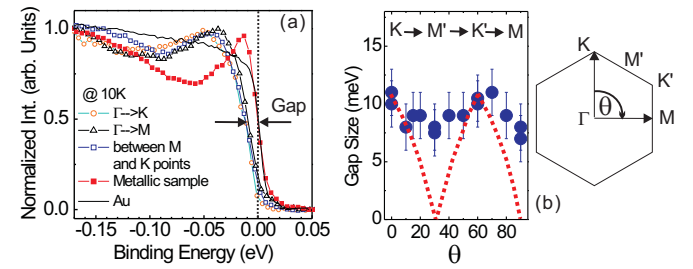


FIG. 3: **Gap Anisotropy:** (a) High energy-resolution (k-integrated on 4% BZ) spectra of $Na_{0.5}CoO_2$ measured at 10K near the folding points along different k-space cuts. Comparison of the spectra with Fermi-edge of Au and metallic $Na_{0.55}CoO_2$ demonstrates the gap in $Na_{0.5}CoO_2$. (b) k-dependence of quasiparticle (leading edge) gap in $K_{0.5}CoO_2$ measured at 10K. Red dots are expected k-dependence of gap in case of nesting occurring *only* along $\Gamma \rightarrow K/K'$ (domain mixing effect) line. The k-space angle θ is defined from $\Gamma \rightarrow K$ to $\Gamma \rightarrow M$ line.

destruction of the a_{1g} Fermi surface only.

Fig. 3(a) shows integrated (momentum window of 0.06 \AA^{-1} 4% of the BZ) low energy spectra near the folding point along $\Gamma \rightarrow M$, $\Gamma \rightarrow K$ and cuts in between. The data are compared to a spectrum from a nearby metallic sample ($x=0.55$). Quasiparticles are seen to be gapped in all high symmetry momentum space cuts. The gap energy Δ varies from 6 to 11 meV. Angular distribution of gap is plotted in Fig-3(b). Gap tends to be larger along $\Gamma \rightarrow K$ cuts.

A hexagonal Fermi surface is observed in nearby dopings ($x=0.3$ or 0.55) at low temperatures but no band-folding is seen. In $x=0.5$ the hexagonal Fermi surface is found to be destroyed at low temperatures by the band folding. Fig-4(a) shows the $n(k)$ map generated with an integration window of 20 meV ($>$ gap size). This shows the topology of the "Fermi surface" around the onset of gap opening. This "Fermi surface" retains hexagonal character except that its volume has changed according to doping. The size of the measured FS at $x=1/2$ doping is found to be special when Na^+ superlattice is considered. In reciprocal space, the primary vector G in hexagonal cell is 2.6 \AA^{-1} . This is much larger than any possible $2k_f$ in any doping over the phase diagram. However, considering the Na^+ lattice ($2 \times \sqrt{3}$ supercell BZ), the shortest vectors G_s are 1.1 and 1.3 \AA^{-1} which is close to the measured value of *average* $2k_f$ for doping in the neighborhood of 0.5. Our results also show that the $\sqrt{3} \times \sqrt{3}$ long-range charge order BZ [8] has no overlap with $x=0.5$ FS (Fig.-4(c)) hence likely not related to the insulating behavior at this particular doping. The Na^+ superstructure imposes a two-fold symmetry on the FS. The Na^+ ionic potential likely enhances nesting conditions ($\vec{Q}_1 \parallel \vec{b}_1$, \vec{Q}_2) along the $\Gamma \rightarrow K/K'$

cuts (Fig.-4(d)). This should then be reflected in the gap and folding behavior. We also consider the domains of the supercell. With a fixed hexagonal matrix there are 3 possible domains for the Na^+ supercell. The domains mix K and K' as well as M and M' but not M with K or M' with K' . Therefore, even in case of complete domain mixing one would expect clear, distinct and different folding and gap behaviors to survive along $\Gamma \rightarrow \text{M}/\text{M}'$ and $\Gamma \rightarrow \text{K}/\text{K}'$ consistent with our observation. In a *conventional* density wave picture [15, 16] gap size is large along the longest straight sections of the FS. Nesting possibility along $\Gamma \rightarrow \text{K}/\text{K}'$ suggests that gap would be larger and band will exhibit stronger folding behavior since ARPES intensity of folding is proportional to nesting strength [16]. It is likely that the effect of the sodium supercell is to flatten out the FS also along $\Gamma \rightarrow \text{M}$ which then leads to a gap. A weaker gap would be expected in such a scenario compared to what was actually observed along M . We note that $\text{Na}_{1/2}\text{CoO}_2$ is not a conventional CDW material like NbSe_3 (band metal) as and other effects (finite correlation gap etc.) are likely at play near the M -point.

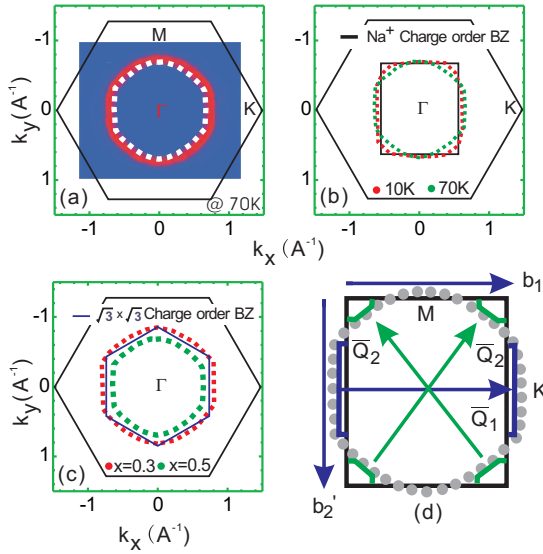


FIG. 4: Particle-hole instabilities on the Fermi surface: Fermi surface reconstruction: Na^+ Charge order vs. $\sqrt{3}x\sqrt{3}$ Co-Charge order (a) Momentum-distribution of quasiparticles (2-color image), $n(\mathbf{k})$, within 20 meV of Fermi energy. The white dots reflect the FS topology. (b) Temperature dependence ($T=10\text{K}$ red dots, 70K green dots) of the "FS topology" in $x=1/2$ samples. The solid black rectangle is the BZ of Na-supercell. Measured FS topology almost coincides with the Na-supercell. (c) The $\sqrt{3}x\sqrt{3}$ Co-Charge order BZ (solid hexagon) has no overlap with $x=0.5$ FS (green dots) but coincides with $x=0.3$ (superconducting doping, red dots) FS. (d) Gray dots are the experimental FS. Green and blue lines are reconstructed FS contours based on experimental folding behavior which is consistent with the geometry of the Na supercell defined by \vec{b}_1' and \vec{b}_2' .

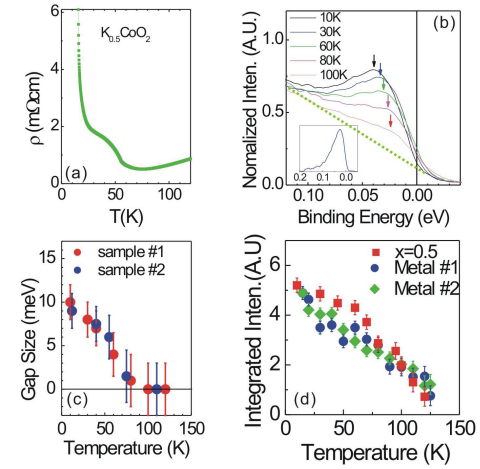


FIG. 5: Gap amplitude and Quasiparticle coherence : Temperature dependence of (a) in-plane *dc*-resistivity, (b) quasiparticle signal along $\Gamma \rightarrow \text{K}$ cut. Inset shows the quasiparticle after linear background subtraction. (c) Evolution of leading-edge gap with temperature. (d) The integrated spectral weight of quasiparticle (coherence) in insulating doping ($x=0.5$, red dots) is compared with the metallic dopings ($x=0.6-0.7$, blue and green points) as a function of temperature. Around 150K spectral coherence (integrated peak intensity) vanishes.

Fig.-5(b) shows the temperature dependence of quasiparticle spectral weight. Quasiparticles get sharper and the energy gap increases as the temperature is lowered. Fig.-5(c) shows the temperature dependence of the charge gap. Temperature dependence of gap viewed as a BCS-like order parameter ($\Delta(T)$) of the transition suggests that its amplitude vanishes beyond 75-80K. This is lower than the SDW transition ($\sim 88\text{K}$) and suggests the gap to be associated with the insulating transitions [2]. Upon further raising the temperature, both the gap size and the spectral weight decrease (beyond thermal broadening). However, the spectral weight does not completely vanish even after the gap has disappeared. Such decrease with rising temperatures is also seen in nearby metallic dopings (Fig-5(d)). ARPES studies have shown that in the coherent transport regime quasiparticles gain significant weight due to enhanced or effective out-of-plane coupling or *c*-axis coherence[17].

Our observation of quasiparticle weight mainly below 150K in $x=1/2$ insulators suggests that even if Na/K layer is ordered well above the room temperature ($\sim 350\text{K}$) the cobalt states are affected by the Na-ion potential after quasiparticles form or gain weight. Therefore, if some approximate nesting is to be operative it can take place only at a similar or lower temperature scale following the growth of quasiparticles. We observe such correlation between the charge gap amplitude and the quasiparticle coherence in insulating cobaltates (Fig.-5).

Similar behavior is seen in cuprate superconductors (SC) where SC-gap opens shortly after the onset of (coherent) quasiparticles which has been ascribed to be due to out-of-plane coupling [18]. In case of cobaltates, instead, it leads to a charge-gap opening as seen in our data which is a *competing instability* with superconductivity. This also argues that the gap we observe is not as one in a band insulator (Slater-type) by the electron count in the new unit cell otherwise it would have appeared at the onset of Na-order and "FS" would have deformed to exactly coincide with the supercell BZ boundary leading to a zero count as in a particle number vanishing phase transitions. This does not happen even down to 10K, so there is no adiabatic continuity to a Slater band insulator phase. It is possible that one of the nesting/modulation vectors (\vec{Q}_1) become operative (longer straight section hence stronger coupling, stronger folding) around 60K (first upturn in resistivity (Fig.5(a)) which nests a good part of the FS but not completely whereas at lower temperatures near 20K both vectors (\vec{Q}_1 , \vec{Q}_2 , possibly also along M) are in effect gapping most of the FS thus leading to resistivity divergence. Such behavior is consistent with NQR data [10].

Density wave modulations in matter form via several different mechanisms. Singularity in the density of states helps realize a density wave state[19]. In a triangular system such singularities in the DOS are expected in case of large and positive t [20]. However, $K_{1/2}CoO_2$ is in the opposite limit namely with a negative sign of hopping ($t < 0$, hole-like band) with a small t_{eff} (~ 16 meV \sim bandwidth(0.15 eV)/9). A more ubiquitous mechanism for developing a density wave modulation is via FS instability. This is the case for $NbSe_3$ and other 1-D metals that exhibit conventional behavior[21]. In most two dimensional materials (2H- $NbSe_2$ etc.[22]) nesting is never complete and FS is partially gapped and the system remains fairly metallic (no insulating divergence). Given the transition temperature (~ 60 K) in cobaltates, the gap size (10 meV) is rather soft compared to many other systems where $\Delta \gg k_B T_c$. Gap closes much faster in cobaltates than it is seen in most CDW systems [21, 22]. The coherence length of the density wave modulation in cobaltate, based on our data, ($v_f \sim 0.5$ eV.Å (Fig.2) : $\xi \sim \hbar v_f / \Delta \sim 10^2$ Å is less than the correlation length of Na charge-order [4] consistent with a density wave induced on the Co plane. Another common mechanism for generating a spectral gap is via valence charge order as argued in [2, 3, 4]. Many oxides indeed exhibit charge-ordering (stripes) due to electron-electron and electron-lattice interactions [1]. Such order typically leads to gap often known as weak correlation gap or pseudogap [1]. No overlap (intersection) of our measured Fermi Surface is observed with the $\sqrt{3}x\sqrt{3}$ cobalt *long-range* charge-order Brillouin zone. However, a combination of FS instability and correlation effects can lead to a *weakly k-dependent* (pseudo-)gap or correlation gap in manganites

in the case of *fluctuating* charge-order[23]. The lack of valence disproportion occurring at the transition [10] has been used to argue for a fluctuating mechanism via intersite Coulomb (V) which likely sets the gap amplitude[24]. This can lead to a finite correlation gap (then the weak k-modulation of the gap reflects the fine FS topological instability effects) in cobaltates. Irrespective of the mechanism of spectral gapping, our results are consistent with IR [7] and SdH measurements[9] where it is argued that almost *entire* FS vanishes at the transition except extremely small left-over pockets (0.25% of the hex-BZ). Such a scenario is consistent with gap and band-folding we observe. The reconstructed corners (Fig-4(d)) are not likely resolved due to finite resolution and weak folding strengths (SdH [9] does not report the exact k-space locations of the pockets hence a detailed comparison is not possible with the dispersion folding (E vs. k) and gap we report by ARPES).

In conclusion, our results suggest that the coupling of quasiparticle states with the crystallized Na layer indeed leads to an intrinsic quantum many-body (correlated) insulating-like low-energy state with weakly k-modulated gap (~ 6 -11 meV) via particle-hole instability on the Fermi surface. Kinematic overlap of the measured Fermi surface is observed with the $\sqrt{3}x\sqrt{3}$ cobalt charge-order Brillouin zone near $x=1/3$ but not at $x=1/2$. The gap opening and quasiparticle signals (coherence) set in at a similar temperature scale which is much smaller than the Na/K charge-order scale and exhibit spectral redistributions over large energy scales in doping and temperature. A comprehensive many-body theory requires to go beyond a conventional one and needs to consider the quasiparticle coherence effects, selective coupling to the superpotential as well as longer-range Coulomb correlations in driving this novel phase transition.

We gratefully acknowledge D.A. Huse, D.H. Lee, M. Lee, P.A. Lee, N.P. Ong, P. Phillips and S. Shastry for discussions. This work is partially supported through NSF-MRSEC (DMR-0213706) grant and the DOE, grant DE-FG02-05ER46200.

-
- [1] M. Imada, A. Fujimori, and Y. Tokura, Rev. Mod. Phys. **70**, 1039 (1998)
 - [2] M. L. Foo *et al.*, Phys. Rev. Lett. **92**, 247001 (2004).
 - [3] H.W. Zandbergen *et al.*, Phys. Rev. B **70**, 024101 (2004).
 - [4] Q. Huang *et. al.*, J. Phys.: Cond. Mat., **16**, 5803 (2004).
 - [5] K. Takada *et al.*, Nature **422**, 53 (2003).
 - [6] Y. Wang *et al.*, Nature **423**, 425 (2003).
 - [7] N.L. Wang *et al.*, Phys. Rev. Lett. **93**, 147403 (2004).
 - [8] O. I. Motrunich, P. A. Lee, Phys. Rev. B **69**, 214516 (2004); *ibid* **70**, 024514 (2004).
 - [9] L. Balicas *et al.* Phys. Rev. Lett. **94**, 236402 (2005).
 - [10] M. Yokoi *et al.*, cond-mat/0506220. J. Bobroff *et al.*, cond-mat/0507514 (2005).
 - [11] M.Z. Hasan *et al.*, Phys. Rev. Lett. **92**, 246402(2004);

- H.B. Yang *et al.*, *ibid* **95**, 146401 (2005).
- [12] D.J. Singh, Phys. Rev. B **61**, 13397 (2000).
- [13] H. Ishida *et al.*, Phys. Rev. Lett. **94**, 196401 (2005).
- [14] M.D. Johannes *et al.*, Phys. Rev. Lett. **93**, 97005 (2004).
- [15] G. Gruner, Density Waves in Solids (Addison-Wesley Pub., Reading, 1994).
- [16] J. Voit *et al.*, Science, **290**, 501 (2000).
- [17] A. Kaminski *et.al.*, Phys. Rev. Lett. **90**, 207003 (2003).
- [18] P.W. Anderson, "The Theory of Superconductivity in High T_c Cuprates" (Princeton Univ. Press, 1997).
- [19] T. M. Rice, G.K. Scott, Phys. Rev. Lett. **35**, 120 (1975).
- [20] B. Kumar, B. S. Shastry, Phys. Rev. B **68**, 104508 (2003).
- [21] J. Schafer *et al.*, Phys. Rev. Lett. **87**, 196403 (2001).
- [22] G.-H. Gweon *et al.*, Phys. Rev. Lett. **81**, 886, (1998); Th. Straub *et al.*, Phys. Rev. Lett. **82**, 4504 (1999).
- [23] Y.-D. Chuang *et al.*, Science 292, 1509 (2001).
- [24] T.P. Choy *et al.*, cond-mat/0502164 (2005).